

Assessing Suitability of Various Battery Technologies for Energy Storages

Lithium-ion, Sodium-sulfur and Vanadium Redox Flow Batteries

Martin Vins

Regional Innovation Centre for Electrical
Engineering
Faculty of Electrical Engineering, UWB
Pilsen, Czechia
mvins@rice.zcu.cz

Martin Sirovy

Regional Innovation Centre for Electrical
Engineering
Faculty of Electrical Engineering, UWB
Pilsen, Czechia
sirovy@rice.zcu.cz

Abstract – The different state of the art industry battery technologies for large-scale energy storage applications are analyzed and compared in this paper. Focus has been paid to Lithium-ion, Sodium-sulfur and Vanadium redox flow batteries. The paper introduces employed methodology of the comparison and modeling. Typical case studies have been evaluated to present strong and weak sides of selected technologies on real applications.

Keywords-Battery; Comparisson; Energy Storage; Lithium-ion; Sodium-sulfur; Vanadium Redox Flow

I. INTRODUCTION

There is increasing pressure to integration of the fluctuating renewable energy sources to the energy grids in present. The appropriate integration of the energy storage systems seems to be one of the solutions for fluctuating energy production and consumption. The advantages of using battery energy storage systems (BESS) are in their fast construction, low environmental demands as well as fast response and high efficiency. The number of the working cycles (lifetime) of the BESS as well as its size are strongly dependent on the used technology. Choosing the proper battery technology for specific energy storage requirements is critical. The aim of this paper is to assess the suitability of use of technologically deployable battery technologies which are the Lithium-ion (Li-ion), Sodium-sulfur (NaS) and Vanadium redox flow (VRB) for application in large-scale energy storages based on the predetermined parameters [1].

II. COMPARISSON ASSUMPTIONS

The input electric parameters are the demanded (permanent) power P_{dem} , demanded capacity W_{dem} , maximal power P_{max_dem} and demanded time of maximal power of the energy storage t_{max_dem} which will be explained below [4].

The other input parameter is the expected number of charge/discharge working cycles per lifetime of the storage n_e [4].

The future system costs are calculated by equation (1) and are considered as evaluation factor of battery suitability for specific energy storage application [4].

$$N_f = N_i \cdot r(i, L) \quad (1)$$

Where N_f (USD) are the future system costs, N_i (USD) are the investment costs, r (%) is the interest rate for project lifetime, i (%) is the year interest rate and L (year) is the lifetime of the storage [4].

A. Li-ion batteries

Currently the most widespread technology of the BESS. For the following calculations, it is assumed that the battery blocks at the nominal output current $I_t = 1$ pu (per unit) have nominal output power P (MW) and nominal capacity W (MWh). A nominal power to capacity ratio is assumed as 1/1 (power (MW) is equal to capacity (MWh)). A battery temperature control system is also assumed. Thus, it is possible to charge and discharge the battery multiples of the I_t (pu), thereby the battery power is increasing as shown in the Table I. [3].

TABLE I. OVERLOADING OF THE LI-ION BATTERIES

I_t (pu)	P (MW)	W (MWh)	Discharge time (h)
1	1	1	1
2	2	1	0.5
3	3	1	0.33

Loading of the battery with the multiples I_t as well as its deep discharge shorten the battery lifetime [3].

For following dependencies is assumed chemical structure LiFePO_4 . The effect of the value of the I_t on the number of working cycles n is described in the following equation (2) [3].

$$n = 5.6271 \cdot I_t^2 - 259.45 \cdot I_t + 253.82 + x \quad (2)$$

The effect of the depth of discharge DoD (%) on the number of the working cycles n is shown in the following equation (3), where x is the number of the working cycles of the specific battery system at $DoD = 100$ % and nominal $I_t = 1$ pu (same as in the equation (2)) [3].

$$n = 5.6911 \cdot DoD^2 - 1090.3 \cdot DoD + 52119 + x \quad (3)$$

These factors lead to the lifetime model shown in the Fig. 1. where x is set demonstratively to 2,500 [3].

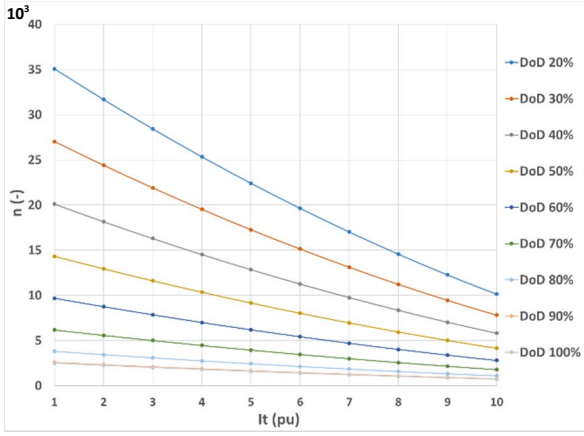


Figure 1. Lifetime model of the Li-ion battery

B. NaS batteries

Currently the only manufacturer is the Japanese company NGK. Due to no manufacturer's variation the x is permanently considered as 4,500 according to [6].

For sodium-sulfur batteries, it is assumed that the battery blocks at the nominal output current $I_t = 1$ pu have nominal output power P (MW) and nominal capacity W (MWh). A nominal power to capacity ratio is assumed as 1/6 (power (MW) is six times lower than capacity (MWh)). It is also assumed that the system is structurally capable of delivering a constant output current $I_t \leq 1$ (excluding short-term overloads described below) [6].

The influence of the DoD on the number of working cycles n is shown in the following equation (4) [6].

$$n = 87,495 \cdot DoD^{-0.645} \quad (4)$$

NaS batteries can be overloaded according to the following equation (5) [2].

$$t_{max} = 30.425 \cdot e^{-1.395m} \quad (5)$$

Where t_{max} is the possible time of the overloading to the m times of the nominal power P [2].

The effect of overloading on shortening lifetime remain unknown and is therefore not included in the following calculations [2], [6].

C. Vanadium redox flow batteries

For vanadium redox flow batteries, it is assumed that the battery blocks at the nominal output current $I_t = 1$ pu have nominal output power P (MW) and nominal capacity W (MWh). A nominal power to capacity ratio is assumed as 1/5 (power (MW) is five times lower than capacity (MWh)), but this ratio may be changed. It is also assumed that the system is structurally capable of delivering an output current $I_t \leq 1$ [5].

The lifetime of a VRB is dependent on construction factors (e.g. membrane lifetime), is not affected by the I_t or the DoD . The lifetime is considered as 25 years and the number of working cycles is considered as 12,000 according to the technical specifications of RedT [5].

This work was supported by the Technology Agency of the Czech Republic within the project No. TN01000007.

III. OPTIMAL BATTERY SIZING

A. Optimal Li-ion battery sizing calculation

The determination of the optimal DoD and I_t is based on the block diagram shown in the Fig. 2. [3], [4].

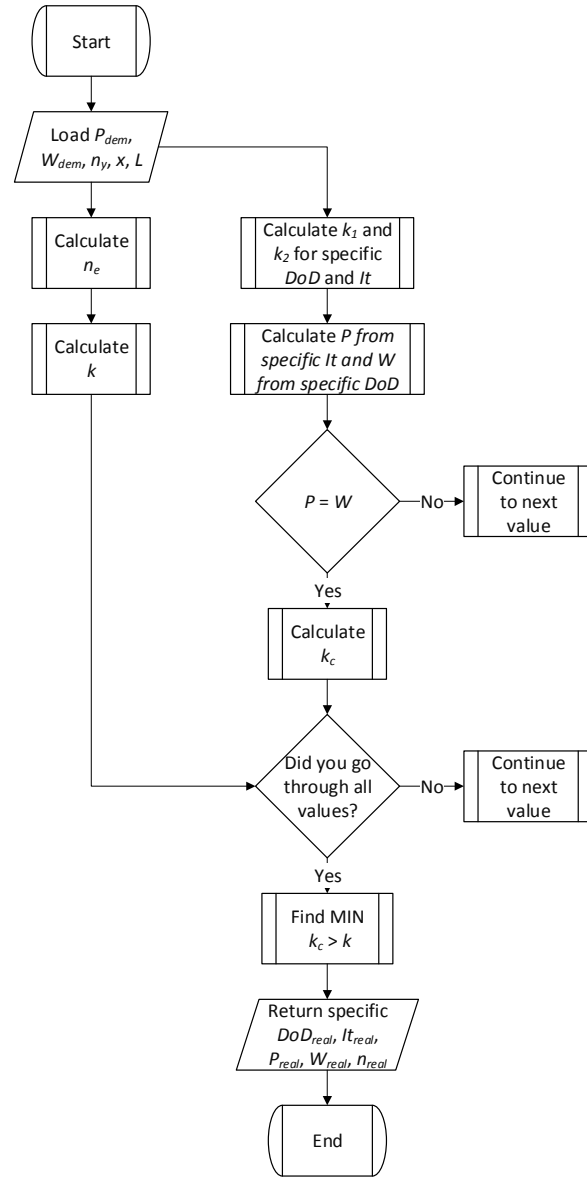


Figure 2. Block diagram of Li-ion sizing calculation

After calculation of the expected number of working cycles over the lifetime n_e , coefficient k is calculated, what indicates the relative change in the number of working cycles from the initial state x at $DoD = 100\%$ and $I_t = 1$ pu [3], [4].

$$k = n_e/x \quad (6)$$

At the same time, the coefficients k_1 for $I_t = 0.1 - 4$ pu are calculated in steps of 0.0025 and k_2 for $DoD = 10 - 100\%$ in steps of 0.05% as shown in equations (7) and (8) [3], [4].

$$k_1 = \frac{5.6271 \cdot I_t^2 - 259.45 \cdot I_t + 253.82 + x}{x} \quad (7)$$

$$k_2 = \frac{5.691 \cdot DoD^2 - 1090.3 \cdot DoD + 52,12 + \lambda}{x} \quad (8)$$

Since the I_t is associated with the P and the DoD with the W , the demanded power P_{dem} is calculated for each I_t and the corresponding demanded capacity to each DoD as shown in the equations (9) and (10) [3], [4].

$$P = P_{dem}/I_t \quad (9)$$

$$W = W_{dem}/DoD \quad (10)$$

Because of the link between power and capacity defined in Chapter II. the matches are found between the calculated power alternative P and the calculated capacity alternative W [3], [4].

When a match is found, the coefficient k_c (-) is calculated from coefficients k_1 (-) and k_2 (-) of the corresponding powers and capacities as shown in the equation (11) [3], [4].

$$k_c = k_1 \cdot k_2 \quad (11)$$

Subsequently, all calculated coefficients k_c are compared with coefficient k and the lowest higher (than k) coefficient k_c is selected [3], [4].

$$MIN k_c > k \quad (12)$$

Then the real system power P_{real} , the real system capacity W_{real} , the optimal DoD_{real} , the optimal I_{treal} and the real number of working cycles n_{real} are expressed from k_c , k_1 and k_2 respectively [3], [4].

B. Optimal NaS battery sizing calculation

If the demanded overloading P_{max_dem} is considered the P_{dem} is adjusted to the P_{dem_upg} according to the block diagram shown in the Fig. 3. Where t_{max_dem} is the demanded time of the overload [2], [4], [6].

The t_{max} is calculated according to equation (5) and the m calculation is shown in the equation (13) [2], [4], [6].

$$m = P_{max_dem}/P_{dem} \quad (13)$$

If the $t_{max_dem} > t_{max}$, the t_{max} is calculated for all $m = 1 - 5$ in steps of 0.01.

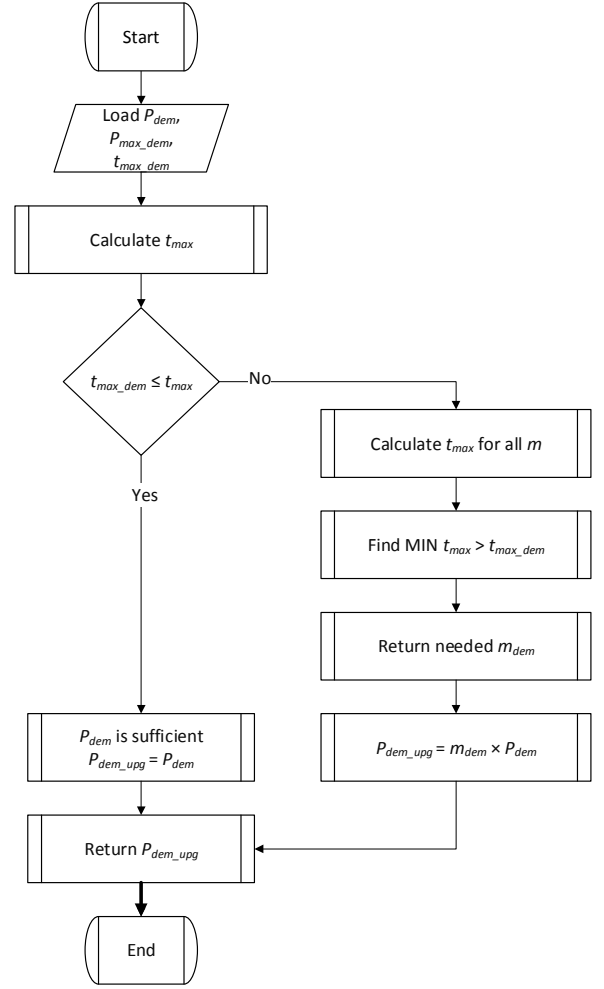


Figure 3. Block diagram of NaS overload sizing calculation

The optimal I_t and DoD are calculated the comparable way to Li-ion batteries. It is based on the block diagram shown in the Fig. 4. [2], [4], [6].

Because the effect of overloading on the battery lifetime is unknown the coefficient k_1 is set permanently to 1. The calculation of the coefficient k_2 is shown in the equation (14) [2], [4], [6].

$$k_2 = \frac{87,495 \times DoD^{-0,645}}{4,500} \quad (14)$$

IV. CASE STUDIES

The results for typical applications are presented in the following two case studies. In the first case study the demanded (input) parameters are shown in the Table II., the real (output) parameters are shown in the Table III. and in the Fig. 5. is shown battery technology cost comparison. In the second case study the demanded (input) parameters are shown in the Table IV., the real (output) parameters are shown in the Table V. and in the Fig. 6. is shown battery technology cost comparison.

Presented costs have only tentative meaning with assumed capital costs of Li-ion - 400 USD/kWh (costs per capacity), NaS - 2 500 USD/kW (costs per power) and VRB - 450 USD/kWh (cost per capacity), the operation costs are completely neglected [1].

In the following first case study is the assumed energy storage used for primary regulation reserve covering. Typically, 2 % power of 200 MW coal fired block for maximum of 15 minutes' duration (what leads to capacity 1 MWh) until the boiler reacts.

TABLE II. CASE STUDY OF PRIMARY RESERVE STORAGE – INITIAL STORAGE PARAMETERS

i (%)	n_e (-)	L (year)	P_{dem} (MW)	W_{dem} (MWh)	t_{max} (h)	x_{Li-ion} (-)	x_{NaS} (-)	n_{VRB} (-)
5	10^4	20	4	1	0.15	2,500	4,500	12,000

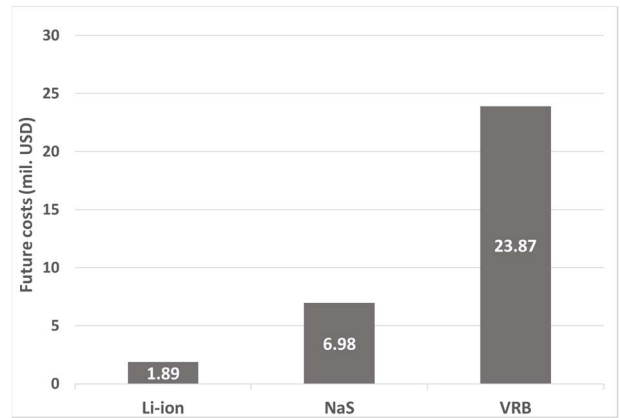


Figure 5. Case study of primary reserve storage

There can be seen that the Li-ion technology seems to be optimal for high power applications. The demanded capacity is 1 MWh as shown in the Table II, but the real capacities of the other technologies are significantly higher to fulfil demanded power because of the output current limitation as shown in the Table III.

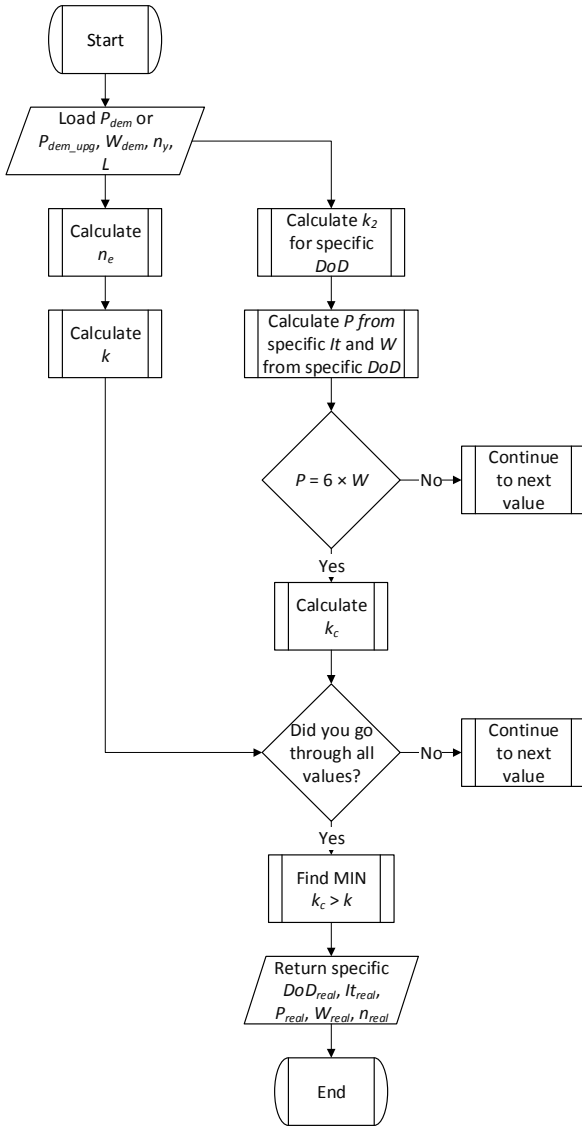


Figure 4. Block diagram of NaS sizing calculation

C. Optimal VRB sizing calculation

Since battery lifetime is not affected by either I_t or DoD , it is optimal to operate this type of battery at $I_t = 1$ and $DoD = 100\%$. For cases where $P_{dem} = 5 \cdot W_{real}$, the depth of discharge and the output current are determined according to the following equations (15) and (16) [4], [5].

$$I_t = \frac{P_{dem}}{(W_{dem}/5)} \cdot DoD \quad (15)$$

if $I_t \leq 1$, otherwise $I_t = 1$

$$DoD = \frac{5 \times P_{dem}}{(W_{dem})} \cdot 100\% \quad (16)$$

if $DoD \leq 100\%$, otherwise $DoD = 100\%$

TABLE III. CASE STUDY OF PRIMARY RESERVE STORAGE – OPTIMAL STORAGE PARAMETERS

	n_e (-)	n_{real} (-)	P_{real} (MW)	W_{real} (MWh)	I_{real} (pu)	DoD_{real} (%)	N_f (mil. USD)
Li-ion	10^4	10,021	1.78	1.78	2.24	56.05	1.89
NaS	10^4	14,744	1.05	6.32	1	15.83	6.98
VRB	10^4	12,000	4	20	1	5	23.87

In the following second case study is assumed energy storage used for fluctuating renewable energy sources compensation (capacity is much higher than power). The capacity is set five times higher than power according to RedT specifications [5].

TABLE IV. CASE STUDY OF HIGH CAPACITY STORAGE – INITIAL STORAGE PARAMETERS

i (%)	n_e (-)	L (year)	P_{dem} (MW)	W_{dem} (MWh)	t_{max} (h)	x_{Li-ion} (-)	x_{NaS} (-)	n_{VRB} (-)
5	10^4	20	4	20	-	2,500	4,500	12,000

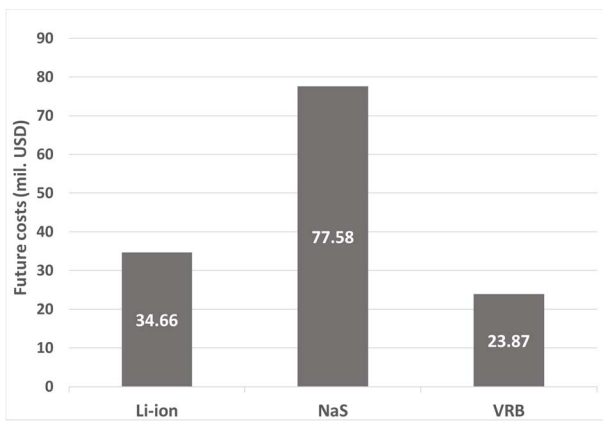


Figure 6. Case study of high capacity storage

There can be seen that the VRB technology seems to be optimal for high capacity and long lifetime applications. The other technologies are affected by their lifetime limitations and due to this fact, they need to be oversized to keep output current appropriately low as shown in the Table V.

TABLE V. CASE STUDY OF HIGH CAPACITY STORAGE – OPTIMAL STORAGE PARAMETERS

	n_e (-)	n_{real} (-)	P_{real} (MW)	W_{real} (MWh)	I_{real} (pu)	DoD_{real} (%)	N_f (mil. USD)
Li-ion	10^4	10,005	32.65	32.65	0.12	61.25	34.66
NaS	10^4	10,096	11.70	70.18	0.34	28.0	77.58
VRB	10^4	12,000	4	20	1	100	23.87

V. DISCUSSION AND CONCLUSION

As mentioned before the capital costs have only tentative meaning. Important is the methodology of mutual comparison of the different battery technologies and optimal sizing of the storages for specific application parameters. It is important to note that the all battery technologies can be used for any storage but there is always one optimal technology from lifetime cost of view.

In the first case study, it can be clearly seen the advantage of the Li-ion batteries primary due to its possibility of overloading and the associated very accurate sizing. Nevertheless, the accurate sizing is not always possible due to manufacturer restrictions (prefabricated capacity of storages, racks or modules).

In the second case study, it can be seen that the costs of VRB are the same like in the first case study but costs of other battery technologies dramatically raised. This is a consequence of considered VRB power to capacity ratio 1/5 which is given by construction of the battery (e.g. membrane surface) and can be different in other VRB systems.

The presented case studies show the suitability of Li-ion batteries for power applications (with lower or equal capacities than powers) and lower number of working cycles, VRB are suitable for capacity applications (capacities are much higher than powers) and higher number of the working cycles. Then NaS batteries are suitable for specific applications with capacities much higher than powers, eventually in the applications where its overloading capability can be used.

ACKNOWLEDGMENT

This work was supported by the Technology Agency of the Czech Republic within the project No. TN01000007.

REFERENCES

- [1] Luo, Xing, et al. "Overview of Current Development in Electrical Energy Storage Technologies and the Application Potential in Power System Operation." *Applied Energy*, vol. 137, 2015, pp. 511–536., doi:10.1016/j.apenergy.2014.09.081.
- [2] Ernesto, Antonio, et al. "Dynamic Modelling of Advanced Battery Energy Storage System for Grid-Tied AC Microgrid Applications." *Energy Storage - Technologies and Applications*, 2013, doi:10.5772/52219.
- [3] Omar, Noshin, et al. "Lithium Iron Phosphate Based Battery – Assessment of the Aging Parameters and Development of Cycle Life Model." *Applied Energy*, vol. 113, 2014, pp. 1575–1585., doi:10.1016/j.apenergy.2013.09.003.
- [4] Tsianikas, Stamatis, et al. "Economic Trends and Comparisons for Optimizing Grid-Outage Resilient Photovoltaic and Battery Systems." *Applied Energy*, vol. 256, 2019, p. 113892., doi:10.1016/j.apenergy.2019.113892.
- [5] "Vanadium Redox Flow Machines - RedT Energy: Industrial Energy Storage Solutions." *RedT Energy | Industrial Energy Storage Solutions*, [cit. 2. 16. 2020], redtenenergy.com/solutions/vanadium_redox_flow_machines/.
- [6] Ngk Insulators. "Specs." *Specs | NAS ENERGY STORAGE SYSTEM: Sodium Sulfur Battery*, [cit. 2. 20. 2020], www.ngk.co.jp/nas/specs/.